

Composite Adaptive Control Barrier Functions for Safety-Critical Systems with Parametric Uncertainty

Mohammadreza Kamaldar*

Department of Mechanical, Aerospace, and Biomedical Engineering
University of South Alabama, Mobile, AL 36688, USA

Abstract

Control barrier functions guarantee safety but typically require accurate system models. Parametric uncertainty invalidates these guarantees. Existing robust methods maintain safety via worst-case bounds, limiting performance, while modular learning schemes decouple estimation from safety, permitting state violations during training. This paper presents the composite adaptive control barrier function (CaCBF) algorithm for nonlinear control-affine systems subject to linear parametric uncertainty. We derive adaptation laws from a composite energy function comprising a logarithmic safety barrier, a control Lyapunov function, and a parameter error term. We prove that CaCBF guarantees the forward invariance of the safe set and the uniform boundedness of the closed-loop system. This safety guarantee holds without requiring parameter convergence. Simulations of adaptive cruise control, an omnidirectional robot, and a planar drone demonstrate the efficacy of the CaCBF algorithm.

1 Introduction

Control barrier functions (CBFs) provide a mathematical mechanism for enforcing safety in autonomous systems [1,2]. By acting as a pointwise filter, a CBF monitors a nominal control signal and modulates it only when the system approaches the boundary of a safe set. This operation renders the safe set forward invariant if the underlying mathematical model accurately represents the physical system. However, physical systems inevitably deviate from their models due to parametric uncertainties, such as variable payloads, unmodeled friction, or aerodynamic drag. This discrepancy challenges the formal safety guarantees of standard CBFs. When the model parameters are incorrect, the calculated safe control input may drive the system into the unsafe region. This uncertainty is typically addressed through two primary paradigms: robust control, bounding the uncertainty, or adaptive control, estimating the parameters.

Robust formulations, such as those established by Jankovic [3] and Zhao et al. [4], maintain safety by enforcing constraints against the worst-case realization of the uncertainty. Recent developments have extended robust CBFs to accommodate complex dynamics. For instance, Buch et al. [5] addressed sector-bounded inputs via second-order cone programs, Xiao and Beta [6] developed formulations for high-order relative degree systems, and Ames et al. [1] introduced input-to-state safety conditions for bounded disturbances. While theoretically rigorous, robustness imposes a geometric cost. As the bounds on parameter uncertainty expand, the subset of control inputs certified as safe contracts. In scenarios with significant uncertainty, this conservatism can render the safe control set empty, causing the solver to fail even when a safe solution physically exists. Furthermore, robust methods compel the system to operate with reduced efficiency, braking earlier, or moving more slowly, regardless of whether the environment is hostile or benign [7].

*Corresponding author: mkamaldar@southalabama.edu

To mitigate this conservatism, researchers utilize online estimation to reduce uncertainty bounds. Modular architectures, such as the robust estimator framework proposed by Das and Burdick [8] or the measurement-robust CBFs developed by Dean et al. [9], employ learning modules to refine parameter estimates over time. These methods separate the estimation process from the control logic. The estimator typically minimizes a prediction error metric, such as the mean squared error between predicted and observed states [10]. While this improves model accuracy, the separation of timescales allows for transient estimation errors independent of the safety boundary. A transient estimation error that occurs while the system is near the boundary can induce a safety violation before the estimator converges.

Integrated approaches attempt to couple estimation and control more tightly. Taylor and Ames [11] introduced Adaptive CBFs to preserve safety under parametric uncertainty, a formulation extended by Lopez and Slotine [12] to handle unmatched uncertainties via certainty equivalence. Other variations include the dynamic penalty functions employed by Xiao et al. [13], the high-order adaptive formulations by Cohen et al. [14], and the auxiliary systems used by Cheng et al. [15] and Zhang et al. [16] for specific applications like electric vehicles and marine vessels. Recently, Cheng et al. [17] combined adaptive CBFs with disturbance observers to manage unstructured noise. Despite these advances, many state-of-the-art methods adopt a modular structure where the adaptation law (e.g., recursive least squares or gradient descent) remains agnostic to the barrier function, as seen in [18, 19]. The learning process reduces parameter error globally rather than prioritizing accuracy in the critical regions where safety is threatened.

Parallel to these efforts, data-driven and nonlinear control techniques seek to tighten robust bounds through experience. Zeng et al. [20] applied composite learning for robotic manipulators, Gutierrez et al. [21] utilized real-time Gaussian Process modeling, and Chriat et al. [22] leveraged reinforcement learning to optimize class- \mathcal{K} functions. Similarly, Barrier Lyapunov Functions (BLFs), explored by Jiang et al. [23] and others [24–26], enforce constraints on tracking errors. However, BLF methods generally require the control architecture to follow a strict backstepping structure [27], which constrains their application to general, optimization-based safety filters for arbitrary nominal controllers.

This paper introduces the *composite adaptive control barrier function* (CaCBF) framework to resolve the conflict between robust conservatism and transient learning risks. Instead of appending an estimator to a fixed controller, we unify parameter estimation and safety certification into a single Lyapunov-based design. We construct a composite energy function that sums a logarithmic barrier potential, representing the proximity to constraint violation, a control Lyapunov function, and a quadratic parameter error term. We then derive an update law that strictly dissipates the total energy. This establishes a feedback loop where the adaptation is driven not only by prediction error but also by the gradient of the safety barrier. As the system approaches the boundary, the effective learning rate adjusts to prioritize the parameters required to maintain safety.

The primary contribution of this work is a unified safety-adaptation architecture. Unlike modular schemes, the CaCBF creates a direct coupling where the risk of violation accelerates the adaptation process. We prove that this formulation guarantees the forward invariance of the safe set for nonlinear systems with linear-in-parameter uncertainties. Crucially, this safety guarantee holds regardless of parameter convergence, eliminating the requirement for persistence of excitation found in classical adaptive control [28, 29]. We validate the framework through three numerical case studies: adaptive cruise control with unknown drag, an omnidirectional robot avoiding obstacles under unknown drift, and a planar drone navigating crosswinds. The results demonstrate that CaCBF achieves set utilization comparable to exact-model methods and outperforms robust baselines, confirming its ability to recover performance in uncertain environments without compromising safety.

Notation. We denote the set of real numbers by \mathbb{R} and the n -dimensional Euclidean space by \mathbb{R}^n . The Euclidean norm is denoted by $\|\cdot\|$. For a symmetric matrix $P \in \mathbb{R}^{n \times n}$, we write $P \succ 0$ (resp. $P \succeq 0$) if P is positive definite (resp. positive semidefinite). Given $P \succ 0$, the weighted Euclidean norm is $\|z\|_P \triangleq \sqrt{z^\top P z}$. The $n \times n$ identity matrix is denoted by I_n .

We denote the limit from the left by $\lim_{\varepsilon \uparrow 0}$ and from the right by $\lim_{\varepsilon \downarrow 0}$. A continuous function $\alpha: [0, a) \rightarrow [0, \infty)$ is of *class \mathcal{K}* if it is strictly increasing and $\alpha(0) = 0$. If $a = +\infty$ and $\lim_{r \rightarrow +\infty} \alpha(r) = +\infty$, it is of *class \mathcal{K}_∞* . In addition, for $b > 0$, a continuous function $\alpha: (-b, a) \rightarrow \mathbb{R}$ is of *extended class \mathcal{K}_e* if $\alpha(0) = 0$ and it is strictly increasing.

Let $h: \mathbb{R}^n \rightarrow \mathbb{R}$, $f: \mathbb{R}^n \rightarrow \mathbb{R}^n$, and $G: \mathbb{R}^n \rightarrow \mathbb{R}^{n \times m}$ be continuously differentiable functions. For $x \in \mathbb{R}^n$, let $\nabla h(x) \triangleq [\frac{\partial h}{\partial x_{(1)}} \cdots \frac{\partial h}{\partial x_{(n)}}]^\top \in \mathbb{R}^n$ denote the gradient vector of h with respect to x . In addition, the Lie derivative of h along f is $L_f h(x) \triangleq \nabla h(x)^\top f(x) \in \mathbb{R}$. Similarly, the Lie derivative of h along G is $L_G h(x) \triangleq \nabla h(x)^\top G(x) \in \mathbb{R}^{1 \times m}$. Finally, for an optimization problem subject to $g(z) \leq 0$, a point z_* is *strictly feasible* if $g(z_*) < 0$.

2 Problem Formulation

Consider the nonlinear control-affine system subject to linear parametric uncertainty given by

$$\dot{x}(t) = f(x(t)) + F(x(t))\theta_* + G(x(t))u(t), \quad (1)$$

where, for all $t \geq 0$, $x(t) \in \mathcal{X} \subseteq \mathbb{R}^n$ is the state, and $u(t) \in \mathcal{U} \subseteq \mathbb{R}^m$ is the control input. The functions $f: \mathcal{X} \rightarrow \mathbb{R}^n$, $F: \mathcal{X} \rightarrow \mathbb{R}^{n \times p}$, and $G: \mathcal{X} \rightarrow \mathbb{R}^{n \times m}$ are known and continuously differentiable, while $\theta_* \in \mathbb{R}^p$ represents a vector of constant, unknown parameters. We impose the following assumption:

(A1) There exists a known constant $\theta_{\max} > 0$ such that $\|\theta_*\| \leq \theta_{\max}$.

Assumption (A1) implies the existence of a known compact convex set

$$\Theta \triangleq \{\theta \in \mathbb{R}^p: \|\theta\| \leq \theta_{\max}\} \quad (2)$$

such that $\theta_* \in \Theta$. The dynamics in (1) capture a class of physical systems characterized by linear-in-parameter uncertainty. Examples include adaptive cruise control, where θ_* represents unknown aerodynamic drag and rolling resistance coefficients; robotic manipulators, where θ_* denotes unknown viscous friction or payload mass; and drone navigation, where θ_* corresponds to unknown crosswind forces. We provide detailed mathematical models and numerical simulations for these specific applications in Section 6.

To encode the safety objective, let the *safe set* $\mathcal{C} \subset \mathcal{X}$ be the superlevel set of a continuously differentiable function $h: \mathcal{X} \rightarrow \mathbb{R}$ defined by

$$\mathcal{C} \triangleq \{x \in \mathcal{X}: h(x) \geq 0\}, \quad (3)$$

and let $\text{bd } \mathcal{C} \triangleq \{x \in \mathcal{X}: h(x) = 0\}$ and $\text{int } \mathcal{C} \triangleq \{x \in \mathcal{X}: h(x) > 0\}$ denote the boundary and interior of \mathcal{C} , respectively.

Let $s: [0, \infty) \times \mathcal{X} \rightarrow \mathcal{X}$ be such that, for all $t \geq 0$, $s(t, x(0))$ is the *trajectory* of (1) corresponding to each initial condition $x(0) \in \mathcal{X}$. The primary objective is to synthesize a control law $u: \mathcal{X} \rightarrow \mathcal{U}$ such that \mathcal{C} is *forward invariant* with respect to the dynamics (1), that is, for all initial conditions $x(0) \in \mathcal{C}$ and all $t > 0$, $s(t, x(0)) \in \mathcal{C}$. Mathematically, a sufficient condition for forward invariance of \mathcal{C} with respect to (1) is provided by Nagumo's Theorem [1], which requires the vector field \dot{x} to point into the set at the boundary, that is, for all $x \in \text{bd } \mathcal{C}$, $\nabla h(x)^\top \dot{x} \geq 0$. Equivalently, if, for all $x \in \text{bd } \mathcal{C}$,

$$\dot{h}(x, u(x)) \geq 0, \quad (4)$$

then, \mathcal{C} is forward invariant with respect to (1). To ensure (4) holds and to regularize the closed-loop behavior within $\text{int } \mathcal{C}$, CBFs enforce the stronger condition that, for all $x \in \mathcal{C}$,

$$\dot{h}(x, u(x)) \geq -\alpha(h(x)), \quad (5)$$

where $\alpha \in \mathcal{K}_e$ is locally Lipschitz. Note that (5) implies that as the state x approaches the boundary of \mathcal{C} (i.e., as $h(x) \downarrow 0$), the permissible rate of decay of the safety margin approaches zero (i.e., $-\alpha(h(x)) \uparrow 0$). Based on the invariance condition (5), we define a CBF for the system (1) as follows.

Definition 1. A continuously differentiable function $h: \mathcal{X} \rightarrow \mathbb{R}$ is a CBF for the system (1) and the safe set \mathcal{C} defined by (3), if there exists a locally Lipschitz function $\alpha \in \mathcal{K}_e$ such that, for all $x \in \mathcal{C}$, the set

$$\mathcal{U}_{\text{cbf}}(x) \triangleq \left\{ \bar{u} \in \mathcal{U} : \dot{h}(x, \bar{u}) \geq -\alpha(h(x)) \right\} \quad (6)$$

is non-empty, where the time derivative \dot{h} is along the trajectories of (1), and is given by

$$\dot{h}(x, \bar{u}) = L_f h(x) + L_F h(x) \theta_* + L_G h(x) \bar{u}. \quad (7)$$

The result connecting Definition 1 to safety is summarized in Theorem 1 in Section 4. Note that (6) relies on \dot{h} , which explicitly depends on the parameter θ_* . Since θ_* is unknown, the set \mathcal{U}_{cbf} is not directly computable. This motivates the design of the composite adaptive CBF in the following section, which simultaneously estimates θ_* , drives the state toward a desired equilibrium, and enforces safety. To characterize the control objective of stabilizing the system states to the origin, we consider the following definition.

Definition 2. A continuously differentiable function $V: \mathcal{X} \rightarrow [0, \infty)$ is a CLF for the system (1) if V is positive definite, radially unbounded, and, there exists $\lambda > 0$ such that, for all $x \in \mathcal{X}$,

$$\inf_{u \in \mathcal{U}} (L_f V(x) + L_F V(x) \theta_* + L_G V(x) u) \leq -\lambda V(x). \quad (8)$$

Note that condition (8) ensures the existence of control inputs that drive the system state to the origin. To ensure the stabilization objective is compatible with the safety constraints, we consider the standard feasibility condition that the equilibrium point lies within the interior of the safe set, i.e., $h(0) > 0$. In the following section, we unify this stabilization objective with the safety guarantees of Definition 1 to derive the proposed composite adaptive framework.

3 Composite Adaptive Control Barrier Functions

In this section, we develop the composite adaptive control barrier function (CaCBF) framework. Unlike robust approaches that rely on static, worst-case bounds, we design an adaptation law that dynamically reduces conservatism while guaranteeing safety. We term this framework *composite* because it unifies three coupled objectives: *safety*, which enforces forward invariance via a logarithmic barrier; *stability*, which drives the state to equilibrium; and *adaptation*, driven by the minimization of an error-estimation cost, to allow the system to operate closer to the safety boundary without violating it.

Let $\hat{\theta}: [0, \infty) \rightarrow \mathbb{R}^p$ be such that, for all $t \geq 0$, $\hat{\theta}(t)$ denotes the instantaneous estimate of the unknown parameter θ_* . In addition, let $\tilde{\theta}: [0, \infty) \rightarrow \mathbb{R}^p$, defined by $\tilde{\theta}(t) \triangleq \hat{\theta}(t) - \theta_*$, denote the instantaneous error. Using Lie derivatives and suppressing time dependence for brevity, the time derivative of h along the trajectories of (1) is given by

$$\dot{h}(x) = L_f h(x) + L_F h(x) \theta_* + L_G h(x) u. \quad (9)$$

Substituting $\theta_* = \hat{\theta} - \tilde{\theta}$ into (9) yields

$$\begin{aligned} \dot{h}(x) &= L_f h(x) + L_F h(x) (\hat{\theta} - \tilde{\theta}) + L_G h(x) u \\ &= \dot{h}_{\hat{\theta}}(x, \hat{\theta}) - \psi(x) \tilde{\theta}, \end{aligned} \quad (10)$$

where $\psi: \mathcal{X} \rightarrow \mathbb{R}^{1 \times p}$ is the *safety regressor* defined by

$$\psi(x) \triangleq L_F h(x), \quad (11)$$

and $\dot{h}_{\hat{\theta}}: \mathcal{X} \times \mathbb{R}^p \rightarrow \mathbb{R}$ is defined by

$$\dot{h}_{\hat{\theta}}(x, \hat{\theta}) \triangleq L_f h(x) + \psi(x) \hat{\theta} + L_G h(x) u, \quad (12)$$

which represents the derivative of the barrier function based on the current parameter estimate $\hat{\theta}$.

To simultaneously ensure safety, promote stability, and bound the parameter error, we introduce the CaCBF, denoted by $V_c: \mathcal{X} \times \mathbb{R}^p \rightarrow \mathbb{R}$ and defined as

$$V_c(x, \hat{\theta}) \triangleq -\ln \left(\frac{h(x)}{1 + h(x)} \right) + \kappa V(x) + \frac{1}{2} \tilde{\theta}^\top \Gamma^{-1} \tilde{\theta}, \quad (13)$$

where h is the CBF used to define the safe set \mathcal{C} in (3), $V: \mathcal{X} \rightarrow [0, \infty)$ is a candidate CLF for the system (1), $\kappa > 0$ is a weighting parameter, and $\Gamma \in \mathbb{R}^{p \times p}$ is a positive-definite adaptation gain matrix. Note that V_c contains a logarithmic barrier function. This construction relies on the property that the barrier term becomes unbounded as the system approaches the safety boundary, that is,

$$\lim_{x \rightarrow \text{bd } \mathcal{C}} \ln \left(\frac{h(x)}{1 + h(x)} \right) = -\infty.$$

Consequently, if V_c remains bounded along the trajectories of (1), the state x is guaranteed to remain within the safe set \mathcal{C} . This implication is formally established in Theorem 3 in Section 4.

We now derive the adaptation law $\dot{\tilde{\theta}}$ by analyzing the time evolution of (13). First, the time derivative of V along the trajectories of (1) is given by

$$\begin{aligned} \dot{V}(x) &= L_f V(x) + L_F V(x) \theta_* + L_G V(x) u \\ &= \dot{V}_{\hat{\theta}}(x, \hat{\theta}) - \phi(x) \tilde{\theta}, \end{aligned} \quad (14)$$

where $\phi: \mathcal{X} \rightarrow \mathbb{R}^{1 \times p}$ is the *stability regressor* defined by

$$\phi(x) \triangleq L_F V(x), \quad (15)$$

and $\dot{V}_{\hat{\theta}}: \mathcal{X} \times \mathbb{R}^p \rightarrow \mathbb{R}$ is defined by

$$\dot{V}_{\hat{\theta}}(x, \hat{\theta}) \triangleq L_f V(x) + \phi(x) \hat{\theta} + L_G V(x) u, \quad (16)$$

which represents the time derivative of the CLF based on the current parameter estimate $\hat{\theta}$. Differentiating the composite energy (13) along the trajectories of (1) yields

$$\dot{V}_c(x, \hat{\theta}) = -\frac{\dot{h}(x)}{h(x)(1 + h(x))} + \kappa \dot{V}(x) + \tilde{\theta}^\top \Gamma^{-1} \dot{\tilde{\theta}}. \quad (17)$$

Since θ_* is constant, it follows that $\dot{\tilde{\theta}} = \dot{\hat{\theta}}$. Thus, substituting (10) and (14) into (17) yields

$$\begin{aligned} \dot{V}_c(x, \hat{\theta}) &= -\frac{\dot{h}_{\hat{\theta}}(x, \hat{\theta}) - \psi(x) \tilde{\theta}}{h(x)(1 + h(x))} + \kappa (\dot{V}_{\hat{\theta}}(x, \hat{\theta}) - \phi(x) \tilde{\theta}) + \tilde{\theta}^\top \Gamma^{-1} \dot{\tilde{\theta}} \\ &= -\frac{\dot{h}_{\hat{\theta}}(x, \hat{\theta})}{h(x)(1 + h(x))} + \kappa \dot{V}_{\hat{\theta}}(x, \hat{\theta}) - \tilde{\theta}^\top \Gamma^{-1} \left(\kappa \Gamma \phi(x)^\top - \frac{\Gamma \psi(x)^\top}{h(x)(1 + h(x))} - \dot{\tilde{\theta}} \right), \end{aligned} \quad (18)$$

where the terms in the parenthesis capture the sign-indefinite effect of parameter uncertainty on both safety and stability. We design $\dot{\hat{\theta}}$ to not only cancel these terms but also minimize the estimation error.

Define the instantaneous estimation error $e: \mathcal{X} \times \mathbb{R}^p \rightarrow \mathbb{R}^n$ by

$$e(x, \hat{\theta}) \triangleq \dot{x} - \left(f(x) + F(x)\hat{\theta} + G(x)u \right), \quad (19)$$

which represents the discrepancy between the measured or estimated state derivative and the estimated state derivative using the current parameter estimate $\hat{\theta}$. Substituting (19) into (19) yields

$$e(x, \hat{\theta}) = -F(x)\tilde{\theta}. \quad (20)$$

To minimize the magnitude of e , we incorporate a gradient descent term based on the instantaneous estimation-error cost $J: \mathcal{X} \times \mathbb{R}^p \rightarrow [0, \infty)$, defined as $J(x, \hat{\theta}) = \frac{1}{2}\|e(x, \hat{\theta})\|^2$. Treating the measured state derivative \dot{x} as independent of $\hat{\theta}$, the gradient of J is derived from (20) as follows:

$$\begin{aligned} \frac{\partial J(x, \hat{\theta})}{\partial \hat{\theta}} &= \left(\frac{\partial e(x, \hat{\theta})}{\partial \hat{\theta}} \right)^\top \frac{\partial J(x, \hat{\theta})}{\partial e(x, \hat{\theta})} \\ &= \left(\frac{\partial}{\partial \hat{\theta}} (-F(x)\tilde{\theta}) \right)^\top e(x, \hat{\theta}) \\ &= -F(x)^\top e(x, \hat{\theta}). \end{aligned} \quad (21)$$

To eliminate the sign-indefinite terms inside the parentheses of (18), we design an adaptation law that explicitly cancels the safety and stability regressors while injecting a gradient update driven by the estimation error (21). Furthermore, to ensure Assumption (A1) is satisfied, we apply a projection operator. Specifically, the parameter update law is given by

$$\dot{\hat{\theta}}(x, \hat{\theta}) = \mathcal{P}_\Theta \left(\Gamma \left(\kappa \phi(x)^\top - \frac{\psi(x)^\top}{h(x)(1+h(x))} + \gamma F(x)^\top e(x, \hat{\theta}) \right), \hat{\theta} \right), \quad (22)$$

where $\hat{\theta}(0) \in \Theta$, $\gamma \geq 0$ is the adaptation gain, and $\mathcal{P}_\Theta: \mathbb{R}^p \times \mathbb{R}^p \rightarrow \mathbb{R}^p$ is a smooth projection operator that confines $\hat{\theta}$ to the known set Θ , and is defined as

$$\mathcal{P}_\Theta(\tau, \hat{\theta}) \triangleq \begin{cases} \tau, & \|\hat{\theta}\| < \theta_{\max} \text{ or } \hat{\theta}^\top \tau \leq 0, \\ \tau - \Gamma \frac{\hat{\theta}^\top \tau}{\hat{\theta}^\top \Gamma \hat{\theta}} \hat{\theta}, & \text{otherwise,} \end{cases} \quad (23)$$

where $\tau \in \mathbb{R}^p$. The projection operator $\mathcal{P}_\Theta(\tau, \hat{\theta})$ modifies the update direction τ only when the estimate reaches the boundary of Θ (i.e., $\|\hat{\theta}\| = \theta_{\max}$) and the update direction τ points outside the set Θ (i.e., $\hat{\theta}^\top \tau > 0$). To satisfy the Lyapunov dissipation property with a general positive-definite gain matrix $\Gamma \succ 0$, the projection is defined as an orthogonal projection onto the tangent plane of the boundary with respect to the Γ^{-1} -weighted Euclidean metric used in (13). As shown in Lemma 1 in the next section, for all $\tau \in \mathbb{R}^p$, \mathcal{P}_Θ satisfies the projection property

$$\tilde{\theta}^\top \Gamma^{-1} (\mathcal{P}_\Theta(\tau) - \tau) \leq 0. \quad (24)$$

Substituting (22) back into (18) and employing (20) and (24) implies that

$$\dot{V}_c(x, \hat{\theta}) \leq -\frac{\dot{h}_{\hat{\theta}}(x, \hat{\theta})}{h(x)(1+h(x))} + \kappa \dot{V}_{\hat{\theta}}(x, \hat{\theta}) - \gamma \|e(x, \hat{\theta})\|^2, \quad (25)$$

which highlights the core advantage of the formulation: the CaCBF evolution depends *only* on known or estimated quantities, while the estimation error provides a nonpositive contribution. Leveraging the decomposition in (25), we synthesize a controller that strictly bounds V_c by constraining the evolution of the estimated safety and stability functions. For instance, imposing the sufficient conditions

$$\dot{h}_{\hat{\theta}}(x, \hat{\theta}) \geq -\alpha(h(x)) \quad \text{and} \quad \dot{V}_{\hat{\theta}}(x, \hat{\theta}) \leq -\lambda V(x) + \delta, \quad (26)$$

where $\lambda, \delta > 0$ and α is a class \mathcal{K} function, transforms (25) into the dissipation inequality

$$\dot{V}_c(x, \hat{\theta}) \leq \frac{\alpha(h(x))}{h(x)(1+h(x))} - \kappa\lambda V(x) - \gamma\|e(x, \hat{\theta})\|^2 + \kappa\delta, \quad (27)$$

where, as proven in Theorem 3 in Section 4, the upper bound ensures that V_c is bounded, thereby guaranteeing safety.

To strictly enforce the conditions in (26) while minimizing control effort and determining the optimal relaxation δ , we formulate the control synthesis as a convex optimization problem that integrates the parameter estimates directly into the constraints. For all $x \in \mathcal{X}$ and all $\hat{\theta} \in \mathbb{R}^p$ evolving according to the adaptation law (22), the control input $u_*: \mathcal{X} \times \mathbb{R}^p$ is the unique solution to the CLF-CBF-QP given by

$$(u_*(x, \hat{\theta}), \delta_*(x, \hat{\theta})) \triangleq \underset{(u, \delta) \in \mathbb{R}^m \times [0, \infty)}{\operatorname{argmin}} \quad \frac{1}{2} u^T R(x) u + \rho \delta^2, \quad (28)$$

$$\text{s.t.} \quad L_f h(x) + \psi(x) \hat{\theta} + L_G h(x) u \geq -\alpha(h(x)), \quad (29)$$

$$L_f V(x) + \phi(x) \hat{\theta} + L_G V(x) u \leq -\lambda V(x) + \delta, \quad (30)$$

where $R: \mathcal{X} \rightarrow \mathbb{R}^{m \times m}$ is positive definite, $\delta \geq 0$ is the relaxation variable for the stability constraint, $\rho > 0$ is the stability-relaxation penalty, and $\lambda > 0$ is the nominal convergence rate of the CLF.

The implementation of the proposed feedback control law is summarized in Algorithm 1, which outlines the computation of the parameter adaptation rate and the optimization-based control input.

4 Closed-Loop Analysis

This section analyzes the closed-loop system formed by the plant dynamics (1), the adaptation law (22), and the adaptive controller (28)–(30). We prove that this feedback interconnection guarantees three essential properties: the feasibility of the optimization, the forward invariance of the safe set, and the boundedness of all system signals.

To ensure the design is well-posed, we impose the following structural assumptions.

- (A2) The safe set \mathcal{C} is non-empty, and h has relative degree 1 with respect to (1); that is, for all $x \in \mathcal{C}$, $L_G h(x) \neq 0$.
- (A3) R is continuous and uniformly positive definite; that is, there exist $\underline{r}, \bar{r} > 0$ such that, for all $x \in \mathcal{C}$, $\underline{r} I_m \preceq R(x) \preceq \bar{r} I_m$.
- (A4) h is a CBF for the system (1) and the safe set \mathcal{C} , and $h(0) > 0$.
- (A5) V is a CLF for the system (1).

Assumption (A2) grants the control input direct authority over the safety barrier. By requiring the relative degree to be 1, we guarantee that the actuator can instantaneously influence the time derivative \dot{h} to steer the system away from the boundary. If this condition fails (i.e., if $L_G h(x) = 0$), the safety constraint

Algorithm 1 CaCBF Algorithm

Design Parameters: Gains $\Gamma \succ 0, \gamma > 0, \kappa > 0$; Weights $R \succ 0, \rho > 0$; Decay Rate $\lambda > 0$

Design Functions: Barrier h , Lyapunov V , Class $\mathcal{K} \alpha$

Sensor Data: System State x , System Response (measured or estimated) \dot{x}

Internal State: Parameter Estimate $\hat{\theta}$

Control & Adaptation: Optimal Control u_* , Parameter Update $\dot{\hat{\theta}}$

```

# Compute Values, Regressors & Estimation Error
1:  $\psi(x) \leftarrow L_F h(x)$ 
2:  $\phi(x) \leftarrow L_F V(x)$ 
3:  $e(x, \hat{\theta}) \leftarrow \dot{x} - (f(x) + F(x)\hat{\theta} + G(x)u_*)$ 

# Evaluate Parameter Adaptation Law
4:  $\tau \leftarrow \Gamma \left[ \kappa \phi(x)^T - \frac{\psi(x)^T}{h(x)(1+h(x))} + \gamma F(x)^T e(x, \hat{\theta}) \right]$ 

# Apply Projection
5:  $\dot{\hat{\theta}} \leftarrow \mathcal{P}_\Theta(\tau, \hat{\theta})$ 

# Solve Adaptive CLF-CBF-QP
6:  $(u_*, \delta_*) \leftarrow \operatorname{argmin}_{(u, \delta)} \frac{1}{2} u^T R(x) u + \rho \delta^2$ 
7: s.t.  $L_f h(x) + \psi(x)\hat{\theta} + L_G h(x)u \geq -\alpha(h(x))$ 
8:  $L_f V(x) + \phi(x)\hat{\theta} + L_G V(x)u \leq -\lambda V(x) + \delta$ 

# Update System
9: Apply  $u_*$  and integrate  $\dot{\hat{\theta}}$ 

```

becomes locally independent of u , potentially rendering the optimization infeasible. We address this specific challenge in the planar drone scenario of Example 3, where the position-based constraints exhibit relative degree 2. In such cases, we employ backstepping techniques [6, 30] to construct extended barrier functions that recover the required relative degree 1 property, thereby restoring direct control authority over the safety condition. Assumption (A3) ensures the optimization problem remains strictly convex. By bounding the eigenvalues of R away from zero, we guarantee a unique optimal solution and prevent the control effort from becoming unbounded. Finally, Assumptions (A4) and (A5) align the safety and stability objectives. Specifically, the condition $h(0) > 0$ implies the target equilibrium lies strictly within the safe set, ensuring the CLF can drive the state to the origin without conflicting with the safety barrier.

The following result, which follows from standard invariance arguments, links the algebraic constraint in Definition 1 to the physical safety of the system. See [1] for a proof.

Theorem 1. Consider the system (1) and the safe set \mathcal{C} . Assume that (A2) is satisfied, and let $h : \mathcal{X} \rightarrow \mathbb{R}$ be a CBF for (1) and \mathcal{C} . In addition, assume that, for all $t \geq 0$, $u(t) \in \mathcal{U}_{\text{cbf}}(x(t))$. Then, \mathcal{C} is forward invariant with respect to (1).

Assumption (A2) guarantees that the gradient ∇h never vanishes on the boundary of the safe set. This regularity condition ensures that $\text{bd } \mathcal{C}$ forms a smooth manifold with a uniquely defined normal vector, a geometric prerequisite for the invariance proof.

Having established the conditions for safety, the next theorem confirms that the control law remains feasible and continuous.

Theorem 2. Consider the CLF-CBF-QP defined in (28)–(30). Assume that (A2) and (A3) are satisfied. Then, the following statements hold:

i) For all $x \in \text{int } \mathcal{C}$ and all $\hat{\theta} \in \mathbb{R}^p$, the CLF-CBF-QP is strictly feasible and has a unique global minimizer.

ii) The optimal control u_* and relaxation δ_* are locally Lipschitz continuous on $\text{int } \mathcal{C} \times \mathbb{R}^p$.

Proof. Let $z \triangleq [u^\top \ \delta]^\top \in \mathbb{R}^{m+1}$. We write the CLF-CBF-QP as

$$z_*(x, \hat{\theta}) \triangleq \underset{z \in \mathbb{R}^{m+1}}{\operatorname{argmin}} \quad \frac{1}{2} z^\top \mathcal{Q}(x) z, \quad (31)$$

$$\text{s.t.} \quad A(x)z \leq b(x, \hat{\theta}), \quad (32)$$

where

$$\mathcal{Q}(x) \triangleq \begin{bmatrix} R(x) & 0 \\ 0 & \rho \end{bmatrix} \in \mathbb{R}^{(m+1) \times (m+1)}, \quad A(x) \triangleq \begin{bmatrix} a_1(x) \\ a_2(x) \end{bmatrix} \in \mathbb{R}^{2 \times (m+1)}, \quad b(x, \hat{\theta}) \triangleq \begin{bmatrix} b_1(x, \hat{\theta}) \\ b_2(x, \hat{\theta}) \end{bmatrix} \in \mathbb{R}^2, \quad (33)$$

and

$$a_1(x) \triangleq [-L_G h(x) \ 0] \in \mathbb{R}^{1 \times (m+1)}, \quad a_2(x) \triangleq [L_G V(x) \ -1] \in \mathbb{R}^{1 \times (m+1)}, \quad (34)$$

$$b_1(x, \hat{\theta}) \triangleq L_f h(x) + L_F h(x) \hat{\theta} + \alpha(h(x)) \in \mathbb{R}, \quad b_2(x, \hat{\theta}) \triangleq -L_f V(x) - L_F V(x) \hat{\theta} - \lambda V(x) \in \mathbb{R}. \quad (35)$$

To prove *i*), let $x \in \text{int } \mathcal{C}$ and $\hat{\theta} \in \mathbb{R}^p$. First, consider the safety constraint $a_1(x)z < b_1(x, \hat{\theta})$. Since (A2) is satisfied, it follows that $a_1(x) \neq 0$, and thus the strict inequality $a_1(x)z < b_1(x, \hat{\theta})$ defines a non-empty, open half-space in \mathbb{R}^m . Therefore, there exists $u_* \in \mathbb{R}^m$ such that, for all $\delta_0 \geq 0$, $z_0 \triangleq [u_*^\top \ \delta_0]^\top$ satisfies the strict safety constraint $a_1(x)z_0 < b_1(x, \hat{\theta})$. Now, let $\delta_1 \triangleq L_G V(x)u_* - b_2(x, \hat{\theta})$ and $z_2 \triangleq [u_*^\top \ \delta_2]^\top$, where $\delta_2 > \max(0, \delta_1)$. It thus follows that $a_2(x)z_2 < b_2(x, \hat{\theta})$. Therefore, since z_2 satisfies both constraints, the CLF-CBF-QP problem is strictly feasible. Moreover, since $\rho > 0$ and (A3) is satisfied, it follows that $\mathcal{Q}(x) \succ 0$, ensuring a unique global minimizer z_* .

To prove *ii*), we use the sensitivity theorem in [31, Theorem 1], which requires the linear independence constraint qualification. Note that \mathcal{Q} , A , and b are composed of smooth vector fields f, F, G and continuously differentiable functions h and V . Since continuously differentiable functions are locally Lipschitz on compact sets, it follows that \mathcal{Q} , A , and b are locally Lipschitz on compact sets. In addition, $R \succ 0$ and $\rho > 0$ imply strict convexity. Next, let $x \in \mathcal{C}$ and $\hat{\theta} \in \mathbb{R}^p$. We prove that the gradients of the active constraints are linearly independent. First, consider the case where exactly one constraint is active. Since (A2) is satisfied, it follows that $a_1(x) \neq 0$. Since, in addition, $a_2(x) \neq 0$, it follows that the active constraint is linearly independent. Second, consider the case where both constraints are active. Let $c_1, c_2 \in \mathbb{R}$, and consider the linear combination $c_1 a_1(x)^\top + c_2 a_2(x)^\top = 0$, which implies

$$c_1 \begin{bmatrix} -L_G h(x)^\top \\ 0 \end{bmatrix} + c_2 \begin{bmatrix} L_G V(x)^\top \\ -1 \end{bmatrix} = \begin{bmatrix} 0 \\ 0 \end{bmatrix}. \quad (36)$$

Since (A2) is satisfied, (36) implies $c_1 = c_2 = 0$. Thus, the gradients of the active constraints are linearly independent. Since all conditions of [31, Theorem 1] are satisfied, z_* is locally Lipschitz continuous, which confirms *ii*) because u_* and δ_* are linear projections of z_* . \square

We now confirm that the projection operator (23) enforces parameter boundedness without corrupting the adaptation direction. This property ensures that the projection mechanism does not counteract the adaptation process.

Lemma 1. Assume that (A1) is satisfied. Then, for all $\tau \in \mathbb{R}^p$ and all $\hat{\theta} \in \Theta$, the projection operator \mathcal{P}_Θ defined in (23) satisfies

$$\tilde{\theta}^\top \Gamma^{-1} (\mathcal{P}_\Theta(\tau, \hat{\theta}) - \tau) \leq 0. \quad (37)$$

Proof. Since (A1) is satisfied, it follows that Θ defined by (2) exists. Let $\tau \in \mathbb{R}^p$ and $\hat{\theta} \in \Theta$. First, consider the case where the projection is inactive, that is, $\|\hat{\theta}\| < \theta_{\max}$ or $\hat{\theta}^\top \tau \leq 0$. In this case, (23) implies that $\mathcal{P}_\Theta(\tau, \hat{\theta}) = \tau$, which confirms (37).

Next, consider the case where the projection is active, that is, $\|\hat{\theta}\| = \theta_{\max}$ and $\hat{\theta}^\top \tau > 0$. It thus follows from (23) that

$$\begin{aligned} \tilde{\theta}^\top \Gamma^{-1} (\mathcal{P}_\Theta(\tau, \hat{\theta}) - \tau) &= \tilde{\theta}^\top \Gamma^{-1} \left(-\Gamma \frac{\hat{\theta}^\top \tau}{\hat{\theta}^\top \Gamma \hat{\theta}} \hat{\theta} \right) \\ &= -\frac{(\tilde{\theta}^\top \hat{\theta})(\hat{\theta}^\top \tau)}{\hat{\theta}^\top \Gamma \hat{\theta}}. \end{aligned} \quad (38)$$

Since $\Gamma \succ 0$ and $\|\hat{\theta}\| = \theta_{\max} > 0$, it follows that $\hat{\theta}^\top \Gamma \hat{\theta} > 0$. Since, in addition, $\hat{\theta}^\top \tau > 0$, it follows from (38) that

$$\operatorname{sgn}(\tilde{\theta}^\top \Gamma^{-1} (\mathcal{P}_\Theta(\tau, \hat{\theta}) - \tau)) = -\operatorname{sgn}(\tilde{\theta}^\top \hat{\theta}). \quad (39)$$

Note that since (A1) is satisfied and $\|\hat{\theta}\| = \theta_{\max}$, the Cauchy-Schwarz inequality implies that

$$\begin{aligned} \tilde{\theta}^\top \hat{\theta} &= (\hat{\theta} - \theta_*)^\top \hat{\theta} \\ &= \|\hat{\theta}\|^2 - \theta_*^\top \hat{\theta} \\ &= \theta_{\max}^2 - \theta_*^\top \hat{\theta} \\ &\geq \theta_{\max}^2 - \|\theta_*\| \|\hat{\theta}\| \\ &\geq 0, \end{aligned} \quad (40)$$

which, combined with (39), confirms (37). \square

The following lemma guarantees that the projection operator confines the parameter estimates to the compact set Θ .

Lemma 2. Assume that (A1) is satisfied. Consider the parameter update law given by (22), where $\hat{\theta}(0) \in \Theta$. Then, for all $t \geq 0$, $\hat{\theta}(t) \in \Theta$.

Proof. Since (A1) is satisfied, it follows that Θ defined by (2) exists. Let $x \in \mathcal{X}$ and $\hat{\theta} \in \mathbb{R}^p$, and define $\tau(x, \hat{\theta}) \triangleq \Gamma(\kappa\phi(x)^\top - \frac{\psi(x)^\top}{h(x)(1+h(x))} + \gamma F(x)^\top e(x, \hat{\theta}))$. For brevity, we omit the arguments and write τ hereafter. First, consider the case where the projection is inactive, that is, $\|\hat{\theta}\| < \theta_{\max}$ or $\hat{\theta}^\top \tau \leq 0$. For the case where $\|\hat{\theta}\| < \theta_{\max}$, it follows that $\hat{\theta} \in \operatorname{int} \Theta$. For the case where $\hat{\theta}^\top \tau \leq 0$, the update direction τ opposes or is orthogonal to $\hat{\theta}$, which is the outward normal vector to boundary of Θ . Thus, it follows from (22) that the time derivative of the squared norm satisfies $\frac{1}{2} \frac{d}{dt} \|\hat{\theta}\|^2 = \hat{\theta}^\top \tau \leq 0$. This implies that $\|\hat{\theta}\|$ is non-increasing, which confirms that $\hat{\theta}$ does not cross the boundary of Θ .

Next, consider the case where the estimate is on the boundary of Θ and the update tries to escape, that is, $\|\hat{\theta}\| = \theta_{\max}$ and $\hat{\theta}^\top \tau > 0$. In this case, the update law is given by the projection

$$\dot{\hat{\theta}} = \tau - \Gamma \frac{\hat{\theta}^\top \tau}{\hat{\theta}^\top \Gamma \hat{\theta}} \hat{\theta}, \quad (41)$$

which is well defined because $\Gamma \succ 0$. Using (41) implies that

$$\begin{aligned}
\frac{1}{2} \frac{d}{dt} \|\hat{\theta}\|^2 &= \hat{\theta}^T \dot{\hat{\theta}} \\
&= \hat{\theta}^T \left(\tau - \Gamma \frac{\hat{\theta}^T \tau}{\hat{\theta}^T \Gamma \hat{\theta}} \hat{\theta} \right) \\
&= \hat{\theta}^T \tau - \left(\frac{\hat{\theta}^T \tau}{\hat{\theta}^T \Gamma \hat{\theta}} \right) \hat{\theta}^T \Gamma \hat{\theta} \\
&= 0,
\end{aligned} \tag{42}$$

which implies that $\|\hat{\theta}\|$ is constant, and thus $\hat{\theta}$ does not cross the boundary of Θ . \square

With the parameter estimates strictly bounded, we turn to the safety of the system. The following theorem proves that the adaptive controller renders the safe set \mathcal{C} forward invariant with respect to the system (1), ensuring the constraints are satisfied for all time.

Theorem 3. Consider the closed-loop system comprising the system (1), the parameter update law (22), and the adaptive control law u_* defined by (28)–(30). Assume that (A1)–(A5) are satisfied, and let $x(0) \in \text{int } \mathcal{C}$ and $\hat{\theta}(0) \in \Theta$. Then, the safe set \mathcal{C} is forward invariant with respect to (1).

Proof. Consider the composite function V_c defined in (13). Taking the time derivative along the closed-loop trajectories yields (18). Note that since (A1) is satisfied and $\hat{\theta}(0) \in \Theta$, Lemma 2 implies that for all $t \geq 0$, $\hat{\theta}(t) \in \Theta$. Therefore, substituting the adaptation law (22) into (18), and using Lemma 1 and (20) implies that

$$\begin{aligned}
\dot{V}_c(x, \hat{\theta}) &= -\frac{\dot{h}_{\hat{\theta}}(x, \hat{\theta})}{h(x)(1+h(x))} + \kappa \dot{V}_{\hat{\theta}}(x, \hat{\theta}) + \gamma \hat{\theta}^T F(x)^T e(x, \hat{\theta}) \\
&\quad - \tilde{\theta}^T \Gamma^{-1} \left(\kappa \Gamma \phi(x)^T - \frac{1}{h(x)(1+h(x))} \Gamma \psi(x)^T + \gamma \Gamma F(x)^T e(x, \hat{\theta}) - \dot{\hat{\theta}} \right) \\
&\leq -\frac{\dot{h}_{\hat{\theta}}(x, \hat{\theta})}{h(x)(1+h(x))} + \kappa \dot{V}_{\hat{\theta}}(x, \hat{\theta}) + \gamma \hat{\theta}^T F(x)^T e(x, \hat{\theta}) \\
&= -\frac{\dot{h}_{\hat{\theta}}(x, \hat{\theta})}{h(x)(1+h(x))} + \kappa \dot{V}_{\hat{\theta}}(x, \hat{\theta}) - \gamma \|e(x, \hat{\theta})\|^2.
\end{aligned} \tag{43}$$

Note that (A4) and (A5) are satisfied. Thus, using (12) and (16), and substituting (29) and (30) into (43) yields

$$\dot{V}_c(x, \hat{\theta}) \leq \frac{\alpha(h(x))}{h(x)(1+h(x))} - \kappa \lambda V(x) - \gamma \|e(x, \hat{\theta})\|^2 + \kappa \delta_*(x, \hat{\theta}). \tag{44}$$

Next, suppose for contradiction, that \mathcal{C} is not forward invariant with respect to (1). Then, there exists $t_1 > 0$ such that $h(x(t_1)) = 0$ and, for all $t \in [0, t_1]$, $h(x(t)) > 0$. It thus follows from (13) that

$$\lim_{t \uparrow t_1} V_c(x(t), \hat{\theta}(t)) = +\infty. \tag{45}$$

Next, note that (44) implies that, for all $t \geq 0$,

$$\dot{V}_c(x(t), \hat{\theta}(t)) \leq \frac{\alpha(h(x(t)))}{h(x(t))(1+h(x(t)))} + \kappa \delta_*(x(t), \hat{\theta}(t)). \tag{46}$$

Since α is Lipschitz, $\alpha(0) = 0$, and $h(t_1) = 0$, there exists a constant $c_\alpha > 0$ such that, for all $t \in [0, t_1]$, $\alpha(h(x(t))) \leq c_\alpha h(x(t))$. Since, in addition, for all $t \in [0, t_1]$, $h(x(t)) \geq 0$, it follows from (46) that, for all $t \in [0, t_1]$,

$$\dot{V}_c(x(t), \hat{\theta}(t)) \leq c_\alpha + \kappa \delta_*(x(t), \hat{\theta}(t)). \quad (47)$$

Next, note that since x is continuous on the closed interval $[0, t_1]$, it follows that, for all $t \in [0, t_1]$, $x(t)$ belongs to a compact set. Moreover, since (A1) is satisfied, Lemma 2 implies that $\hat{\theta}$ is bounded. Furthermore, since (A2) and (A3) are satisfied, part *ii* of Theorem 2 implies δ_* is Lipschitz continuous. It thus follows that $\delta_{\max} \triangleq \sup_{\tau \in [0, t_1]} \delta_*(x(\tau), \hat{\theta}(\tau))$ exists. It thus follows from (47) that, for all $t \in [0, t_1]$,

$$\dot{V}_c(x(t), \hat{\theta}(t)) \leq c_\alpha + \kappa \delta_{\max}. \quad (48)$$

Integrating (48) over the interval $[0, t_1]$ yields

$$V_c(x(t_1), \hat{\theta}(t_1)) \leq V_c(x(0), \hat{\theta}(0)) + t_1(c_\alpha + \kappa \delta_{\max}) < +\infty, \quad (49)$$

which contradicts (45). Thus, for all $t \geq 0$, $h(x(t)) > 0$, which confirms the result. \square

To guarantee the uniform boundedness of all closed-loop signals, we impose the following structural assumption on the system's asymptotic behavior.

(A6) There exists a compact set $\mathcal{S} \subset \mathcal{X}$ containing the origin and a constant $\varepsilon > 0$ such that, for all $x \in \mathcal{X} \setminus \mathcal{S}$ and all $\hat{\theta} \in \Theta$,

$$\lambda V(x) - \delta_*(x, \hat{\theta}) \geq \varepsilon. \quad (50)$$

Assumption (A6) ensures that outside the set \mathcal{S} , the drive for stability λV outpaces the cost of safety δ_* . Physically, the relaxation term δ_* represents the control effort “wasted” to satisfy safety constraints or compensate for parameter errors. By requiring the stability term to dominate, we ensure the controller always retains enough authority to pull the system back toward the origin. This structure is typical of mechanical systems where the CLF grows quadratically, while the uncertainty and safety conflicts grow only linearly or sub-quadratically.

The following proposition identifies sufficient conditions for this property to hold.

Lemma 3. Assume that (A1)–(A3) and (A5) are satisfied, and let $\lambda > 0$ and $u_n: \mathcal{X} \rightarrow \mathbb{R}^m$ be such that, for all $x \in \mathcal{X}$,

$$L_f V(x) + \phi(x) \theta_* + L_G V(x) u_n(x) \leq -\lambda V(x). \quad (51)$$

In addition, assume that there exists $c_u > 0$ such that, for all $x \in \mathcal{X}$,

$$\|u_n(x)\|_{R(x)} \leq c_u \sqrt{V(x)}. \quad (52)$$

Furthermore, assume that there exists $c_F > 0$ such that, for all $x \in \mathcal{X}$, at least one of the following conditions holds:

- i) $\|\phi(x)\| \leq c_F \sqrt{V(x)}$.
- ii) $\|\phi(x)\| \leq c_F V(x)$ and $\lambda > 2c_F \theta_{\max}$.

Then, (A6) is satisfied.

Proof. Note that since (A1) is satisfied, it follows that Θ defined by (2) exists. Let $\hat{\theta} \in \Theta$. Since (A5) is satisfied, using (14) and (51) implies that, for all $x \in \mathcal{X}$,

$$\begin{aligned}\dot{V}_{\hat{\theta}}(x, \hat{\theta}) &= \dot{V}(x) + \phi(x)\tilde{\theta} \\ &\leq -\lambda V(x) + \phi(x)\tilde{\theta} \\ &\leq -\lambda V(x) + \delta_n(x, \hat{\theta}),\end{aligned}\tag{53}$$

where $\delta_n(x, \hat{\theta}) \triangleq \max\{0, \phi(x)\tilde{\theta}\}$. It thus follows that, for all $x \in \mathcal{X}$, the pair $(u_n(x), \delta_n(x, \hat{\theta}))$ satisfies the stability constraint (30). Moreover, since (A2) and (A3) are satisfied, it follows that, for all $x \in \mathcal{X}$, $(u_*(x, \hat{\theta}), \delta_*(x, \hat{\theta}))$ is the optimal solution minimizing the cost (28). It thus follows that, for all $x \in \mathcal{X}$,

$$\begin{aligned}\rho\delta_*(x, \hat{\theta})^2 &\leq \frac{1}{2}\|u_*(x, \hat{\theta})\|_{R(x)}^2 + \rho\delta_*(x, \hat{\theta})^2 \\ &\leq \frac{1}{2}\|u_n(x)\|_{R(x)}^2 + \rho\delta_n(x, \hat{\theta})^2.\end{aligned}\tag{54}$$

Note that, since $\hat{\theta}, \theta_* \in \Theta$, using the triangle inequality $\|\tilde{\theta}\| \leq \|\hat{\theta}\| + \|\theta_*\| \leq 2\theta_{\max}$ implies that, for all $x \in \mathcal{X}$,

$$\delta_n(x, \hat{\theta}) \leq \|\phi(x)\|\|\tilde{\theta}\| \leq 2\|\phi(x)\|\theta_{\max}.\tag{55}$$

Taking the square root of both sides of (54), and dividing by $\sqrt{\rho}$ implies that, for all $x \in \mathcal{X}$,

$$\begin{aligned}\delta_*(x, \hat{\theta}) &\leq \frac{\|u_n(x)\|_{R(x)}}{\sqrt{2\rho}} + \delta_n(x, \hat{\theta}) \\ &\leq \frac{c_u \sqrt{V(x)}}{\sqrt{2\rho}} + 2\theta_{\max}\|\phi(x)\|,\end{aligned}\tag{56}$$

where the last inequality follows from (52) and (55).

First, consider the case where *i*) is satisfied, and it follows from (56) that, for all $x \in \mathcal{X}$,

$$\lambda V(x) - \delta_*(x, \hat{\theta}) \geq \lambda V(x) - \left(\frac{c_u}{\sqrt{2\rho}} + 2c_F\theta_{\max} \right) \sqrt{V(x)},\tag{57}$$

which, since V is radially unbounded, implies that $\lim_{\|x\| \rightarrow \infty} (\lambda V(x) - \delta_*(x, \hat{\theta})) = +\infty$.

Next, consider the case where *ii*) is satisfied, and it follows from (56) that, for all $x \in \mathcal{X}$,

$$\lambda V(x) - \delta_*(x, \hat{\theta}) \geq (\lambda - 2c_F\theta_{\max})V(x) - \frac{c_u}{\sqrt{2\rho}}\sqrt{V(x)},\tag{58}$$

which, since V is radially unbounded and $\lambda > 2c_F\theta_{\max}$, implies that $\lim_{\|x\| \rightarrow \infty} (\lambda V(x) - \delta_*(x, \hat{\theta})) = +\infty$. Therefore, since in both cases *i*) and *ii*), $\lim_{\|x\| \rightarrow \infty} (\lambda V(x) - \delta_*(x, \hat{\theta})) = +\infty$, it follows that, for all $\varepsilon > 0$, there exists a compact level set $\mathcal{S} \subset \mathcal{X}$ such that for all $x \in \mathcal{X} \setminus \mathcal{S}$, $\lambda V(x) - \delta_*(x, \hat{\theta}) \geq \varepsilon$, which confirms (A6). \square

Lemma 3 establishes that for large states, the drive for stability outpaces the relaxation penalties required for safety. Building on this asymptotic dominance, the following theorem guarantees that all closed-loop signals remain uniformly bounded.

Theorem 4. Consider the closed-loop system comprising the system (1), the parameter update law (22), and the adaptive control law u_* defined by (28)–(30). Assume that (A1)–(A6) are satisfied, and let $x(0) \in \text{int } \mathcal{C}$ and $\hat{\theta}(0) \in \Theta$. Then, all closed-loop signals $x, \hat{\theta}, u$, and δ are uniformly bounded.

Proof. Consider the time derivative of V_c . Since (A1) is satisfied, using the derivation in (44) implies that

$$\dot{V}_c(x, \hat{\theta}) \leq \frac{\alpha(h(x))}{h(x)(1+h(x))} - \kappa \left(\lambda V(x) - \delta_*(x, \hat{\theta}) \right). \quad (59)$$

Since α is a Lipschitz class \mathcal{K} function with $\alpha(0) = 0$, there exists a constant $c_\alpha > 0$ such that, for all $r \geq 0$, $\alpha(r) \leq c_\alpha r$. Substituting this into (59) yields:

$$\begin{aligned} \dot{V}_c(x, \hat{\theta}) &\leq \frac{c_\alpha}{1+h(x)} - \kappa \left(\lambda V(x) - \delta_*(x, \hat{\theta}) \right) \\ &\leq c_\alpha - \kappa \left(\lambda V(x) - \delta_*(x, \hat{\theta}) \right), \end{aligned} \quad (60)$$

where the last inequality holds because (A1)–(A5) are satisfied, and thus Theorem 3 implies that, for all $t \geq 0$, $h(x(t)) > 0$.

Next, note that since (A6) is satisfied, it follows from (60) that, for all $x \in \mathcal{X} \setminus \mathcal{S}$ and all $\hat{\theta} \in \Theta$,

$$\dot{V}_c(x, \hat{\theta}) \leq c_\alpha - \kappa \varepsilon. \quad (61)$$

Let $\kappa > \frac{c_\alpha}{\varepsilon}$, and it follows from (61) that, for all $x \in \mathcal{X} \setminus \mathcal{S}$,

$$\dot{V}_c(x, \hat{\theta}) < 0. \quad (62)$$

We now establish the forward invariance of a specific sublevel set. Let $s_0 \triangleq \max_{x \in \mathcal{S}, \hat{\theta} \in \Theta} V_c(x, \hat{\theta})$ and define the sublevel set $\Omega_s \triangleq \{(x, \hat{\theta}) \in \mathcal{X} \times \Theta \mid V_c(x, \hat{\theta}) \leq s\}$, where $s \geq \max\{V_c(x(0), \hat{\theta}(0)), s_0\}$. Since $s \geq s_0$, it follows that, for all $(x, \hat{\theta}) \in \mathcal{X} \setminus \text{int } \Omega_s$, $(x, \hat{\theta}) \in \mathcal{X} \setminus \mathcal{S} \times \Theta$. It thus follows from (62) that Ω_s is forward invariant with respect to (1). Thus, for all $t \geq 0$, $(x(t), \hat{\theta}(t)) \in \Omega_s$, which implies $V_c(t) \leq s$.

Finally, note that since (A5) implies that V is radially unbounded, there exists a class \mathcal{K} function $\underline{\alpha}$ such that, for all $t \geq 0$, $\underline{\alpha}(\|x(t)\|) \leq V(x(t))$. In addition, since (A1) is satisfied, Lemma 1 implies that, for all $t \geq 0$, $V_c(x(t), \hat{\theta}) \geq V(x(t))$. It thus follows that $\underline{\alpha}(\|x(t)\|) \leq V(x(t)) \leq V_c(t) \leq s$. Therefore, for all $t \geq 0$, $\|x(t)\| \leq \underline{\alpha}^{-1}(s)$, which confirms that x is uniformly bounded. Since, in addition, Lemma 2 implies, for all $t \geq 0$, $\hat{\theta}(t) \in \Theta$, it follows that the joint state $(x(t), \hat{\theta}(t))$ evolves within a compact domain. Therefore, since the image of a compact set under a continuous map is compact, part *ii*) of Theorem 2 implies that the control input u_* and relaxation δ_* are uniformly bounded, which confirms the result. \square

5 Comparison with Robust CBF

To quantify the advantage of the adaptive framework, we compare its admissible control space against a standard robust baseline. Let $\theta_e \in \mathbb{R}^p$ represent a fixed parameter estimate. We define the worst-case uncertainty margin σ_{rob} as the maximum possible deviation over the parameter set given by

$$\sigma_{\text{rob}}(x, \theta_e) \triangleq \max_{\vartheta \in \Theta} |L_F h(x)(\vartheta - \theta_e)|. \quad (63)$$

A standard robust CBF (R-CBF) guarantees safety by guarding against the worst-case parameter realization by imposing the conservative constraint

$$L_F h(x) + \psi(x) \theta_e + L_G h(x) u - \sigma_{\text{rob}}(x, \theta_e) \geq -\alpha(h(x)). \quad (64)$$

In contrast, the proposed CaCBF uses the evolving estimate $\hat{\theta}$ to enforce the nominal constraint (29). By swapping the static worst-case margin for a dynamic adaptation process, the CaCBF expands the feasible control space. The following theorem confirms this advantage: it proves that the admissible control set of the adaptive formulation contains the robust set as a subset.

Theorem 5. Assume that (A1) is satisfied, let $\theta_e \in \mathbb{R}^p$ and $\hat{\theta} \in \Theta$. Furthermore, let $\mathcal{U}_{\text{rob}}(x, \theta_e)$ and $\mathcal{U}_{\text{adp}}(x, \hat{\theta})$ denote the sets of admissible control inputs satisfying the R-CBF condition (64) and the CaCBF condition (29), respectively. Then, for all $x \in \mathcal{C}$,

$$\mathcal{U}_{\text{rob}}(x, \theta_e) \subseteq \mathcal{U}_{\text{adp}}(x, \hat{\theta}). \quad (65)$$

Proof. Let $x \in \mathcal{C}$ and $u \in \mathcal{U}_{\text{rob}}(x, \theta_e)$. By definition, u satisfies the robust inequality

$$L_G h(x)u \geq -L_f h(x) - \psi(x)\theta_e - \alpha(h(x)) + \sigma_{\text{rob}}(x, \theta_e). \quad (66)$$

Since $\hat{\theta} \in \Theta$, it follows from the definition of the worst-case margin that $\sigma_{\text{rob}}(x, \theta_e) \geq |\psi(x)(\hat{\theta} - \theta_e)| \geq \psi(x)(\theta_e - \hat{\theta})$. It thus follows from (66) that

$$\begin{aligned} L_G h(x)u &\geq -L_f h(x) - \psi(x)\theta_e - \alpha(h(x)) + \psi(x)(\theta_e - \hat{\theta}) \\ &= -L_f h(x) - \psi(x)\hat{\theta} - \alpha(h(x)), \end{aligned} \quad (67)$$

which matches (29). Thus, $u \in \mathcal{U}_{\text{adp}}(x, \hat{\theta})$, which confirms the inclusion (65). \square

Equation (65) confirms that CaCBF recovers control authority that the R-CBF approach would otherwise discard. R-CBF shrinks the safe set, guarding against the worst possible parameter configuration at every instant. In contrast, CaCBF uses the current parameter estimate. Rather than relying on a static, worst-case margin, CaCBF relies on the adaptation mechanism to correct errors online. This allows the system to compensate for uncertainty dynamically, granting access to a larger set of safe control inputs. Figure 1 provides a geometric interpretation of this result. It illustrates that, for each $x \in \mathcal{C}$, $\theta_e \in \mathbb{R}^p$, and $\hat{\theta} \in \Theta$, the robust safe control set $\mathcal{U}_{\text{rob}}(x, \theta_e)$, computed using the fixed estimate θ_e , is nested within the adaptive safe control set $\mathcal{U}_{\text{adp}}(x, \hat{\theta})$. As the estimate $\hat{\theta}$ converges to the true parameter, the dashed boundary of $\mathcal{U}_{\text{adp}}(x, \hat{\theta})$ expands to recover the true safe control set $\mathcal{U}_{\text{cbf}}(x)$. Equation (65) confirms that CaCBF recovers control authority that the robust formulation discards.

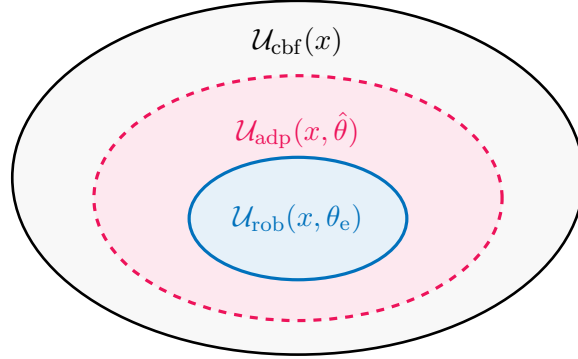


Figure 1: Geometric interpretation of Theorem 5 at each $x \in \mathcal{C}$, $\theta_e \in \mathbb{R}^p$, and $\hat{\theta} \in \Theta$. The conservative robust safe control set $\mathcal{U}_{\text{rob}}(x, \theta_e)$ (inner, blue) is nested within the adaptive safe control set $\mathcal{U}_{\text{adp}}(x, \hat{\theta})$ (middle, red, dashed). The adaptive set expands toward the true safe control set $\mathcal{U}_{\text{cbf}}(x)$ (outer, solid) as $\hat{\theta}$ converges to the true parameter θ_* .

6 Numerical Examples

We illustrate the proposed CaCBF framework through numerical simulations on three distinct dynamical systems. First, we use an adaptive cruise control problem to illustrate and quantify the benefits of adaptation,

showing how the CaCBF recovers control authority that a standard R-CBF would discard. We then broaden the scope to include a quadrotor drone and an inverted pendulum, demonstrating that the safety guarantees hold across diverse uncertain physical systems.

Example 1. *Adaptive cruise control with unknown resistance force.* We illustrate the framework using an adaptive cruise control problem based on the point-mass model in [2]. The ego vehicle must follow a lead vehicle that executes a variable-velocity profile

$$v_\ell(t) \triangleq \begin{cases} 10, & 0 \leq t < 25, \\ 14, & 25 \leq t < 50, \\ 18, & 50 \leq t < 75, \\ 15, & 75 \leq t < 100, \end{cases} \quad (68)$$

while maintaining a desired cruising speed $v_d \triangleq 26$ m/s and a safe time headway $\tau_d \triangleq 1.8$ s. We define the safety set \mathcal{C} via the zeroing barrier function

$$h(x) = d - 1.8v. \quad (69)$$

Let the state be $x = [v \ d]^\top \in \mathbb{R}^2$, where v is the ego velocity and d is the following distance. The system evolves according to

$$\dot{x} = \begin{bmatrix} 0 \\ v_\ell - v \end{bmatrix} + \begin{bmatrix} -\frac{1}{\bar{m}} & -\frac{v}{\bar{m}} & -\frac{v^2}{\bar{m}} \\ 0 & 0 & 0 \end{bmatrix} \theta_* + \begin{bmatrix} \frac{1}{\bar{m}} \\ 0 \end{bmatrix} u, \quad (70)$$

where $\bar{m} \triangleq 1650$ kg is the mass, u is the wheel force, and $\theta_* = [7 \ 6 \ 5]^\top$ captures the unknown coefficients for rolling resistance and aerodynamic drag. The initial conditions are $v(0) = 25$ m/s and $d(0) = 60$ m. To respect traction limits and passenger comfort, we bound the control input such that, for all $t \geq 0$,

$$-0.25\bar{m}g \leq u(t) \leq 0.25\bar{m}g, \quad (71)$$

where $g = 9.81$ m/s² is the gravitational acceleration.

We first implement the proposed CaCBF. We select the CLF candidate $V(x) = (v - v_d)^2$ with a nominal convergence rate $\lambda = 2$. Inserting the dynamics (70) and the Lie derivatives calculated with the estimate $\hat{\theta}$ into the CLF-CBF-QP (28)–(30) yields, for all $x \in \mathbb{R}^n$ and $\hat{\theta} \in \mathbb{R}^p$, the optimization

$$(u_*(x, \hat{\theta}), \delta_*(x, \hat{\theta})) = \underset{(u, \delta) \in \mathbb{R} \times [0, \infty)}{\operatorname{argmin}} \quad \frac{1}{2}u^2 + \rho\delta^2, \quad (72)$$

$$\text{s.t.} \quad v_\ell - v + \frac{1.8(\zeta(v)^\top \hat{\theta} - u)}{\bar{m}} \geq 1.8v - d, \quad (73)$$

$$\frac{2(v_d - v)(\zeta(v)^\top \hat{\theta} - u)}{\bar{m}} \leq -2(v - v_d)^2 + \delta, \quad (74)$$

where the regressor is $\zeta(v) \triangleq [1 \ v \ v^2]^\top$, the penalty weight is $\rho = 10^3$, and the class \mathcal{K} function is the identity function $\alpha(h(x)) = h(x)$. We set the bounds and gains as $\theta_{\max} = 20$, $\hat{\theta}(0) = 0$, $\Gamma = \operatorname{diag}(10^4, 10^3, 10^2)$, $\gamma = 10^2$, and $\kappa = 1$.

For comparison, we implement a standard R-CBF. We use a fixed parameter estimate $\theta_e = \hat{\theta}(0) = 0$. To guarantee safety against all $\theta \in \Theta$, the robust controller subtracts a margin proportional to the worst-case uncertainty. Substituting (70) into the robust condition (64) generates the constraint

$$v_\ell - v - \frac{1.8}{\bar{m}} (\|\zeta(v)\| \theta_{\max} + u) \geq 1.8v - d, \quad (75)$$

which replaces (73) in the QP formulation.

Figure 2 shows the cost of this robustness. The R-CBF exhibits conservatism, applying mechanical braking far earlier than necessary. In contrast, the adaptive controller learns the resistance profile, allowing it to account for drag forces within the safety constraints. This reduces the mechanical braking effort and allows the vehicle to close the gap to the lead vehicle more aggressively than the robust trajectory, while maintaining strict safety.

We quantify performance using three metrics: the minimum safety margin $h_{\min} \triangleq \min_{t \in [0, T]} h(x(t))$, which tracks the closest approach to the boundary and where $T = 100$ s is the total simulation duration; the total braking effort $E_{\text{brake}} \triangleq \int_0^T |\min(0, u(t))| dt$, which measures the mechanical energy spent on deceleration; and the time-averaged clearance $\eta \triangleq \frac{1}{T} \int_0^T h(x(t)) dt$. A lower η indicates that the controller operates closer to the constraint, reflecting reduced conservatism. We evaluate performance using three quantitative metrics: the minimum safety margin $h_{\min} \triangleq \min_t h(x(t))$, the total braking effort $E_{\text{brake}} \triangleq \int_0^T |\min(0, u(t))| dt$, and the time-averaged clearance $\eta \triangleq \frac{1}{T} \int_0^T h(x(t)) dt$. The simulation results highlight the efficiency of the adaptive approach. While both controllers require comparable mechanical braking effort $E_{\text{brake}} \approx 1.40 \times 10^4$ N·s, the robust controller achieves this by maintaining a large, conservative buffer of $h_{\min} = 2.81$ m. In contrast, the CaCBF safely utilizes the available space, approaching within 0.17 m of the boundary. This reduction in conservatism is further confirmed by the average clearance metric: the robust controller operates with a wide margin ($\eta = 6.27$ m), whereas the adaptive formulation reduces this to $\eta = 0.53$ m, demonstrating that the system recovers nearly all the safe operating space that the robust controller discards. Furthermore, the robust controller's high average clearance $\eta = 6.03$ m contrasts sharply with the adaptive result $\eta = 0.32$ m, demonstrating that the CaCBF recovers nearly all the safe operating space that the robust controller discards. \diamond

Example 2. *Omnidirectional robot navigation with unknown drift.* We illustrate the CaCBF framework using a planar navigation problem for an omnidirectional robot modeled as a kinematic point mass. Let the state be $x = [p_x \ p_y]^T \in \mathbb{R}^2$, where $p_x \in \mathbb{R}$ and $p_y \in \mathbb{R}$ are the horizontal and vertical positions, respectively. The system evolves according to

$$\dot{x} = u + \theta_*, \quad (76)$$

where $u = [v_x \ v_y]^T$ is the velocity control input, and $v_x \in \mathbb{R}$ and $v_y \in \mathbb{R}$ are the horizontal and vertical velocity, respectively. In addition, $\theta_* = [0.3 \ -0.2]^T$ represents the unknown wind or drift velocity. The initial condition is $x(0) = [0 \ 5]^T$. The objective is to navigate from $x(0)$ to a target $x_d \triangleq [10 \ 5]^T$ while avoiding a circular obstacle centered at $x_{\text{obs}} \triangleq [5 \ 5]^T$ with radius $r_{\text{obs}} \triangleq 4.5$ m. We define the safety set \mathcal{C} via the distance-based barrier function

$$h(x) = \|x - x_{\text{obs}}\|^2 - r_{\text{obs}}^2. \quad (77)$$

To respect actuator limits, we bound the control input such that, for all $t \geq 0$,

$$\|u(t)\| \leq 2 \text{ m/s}. \quad (78)$$

We first implement the proposed CaCBF. We select the CLF candidate $V(x) = \|x - x_d\|^2$ with a nominal convergence rate $\lambda = 1$. The Lie derivatives are $L_f h(x) = 0$ and $L_G h(x) = 2(x - x_{\text{obs}})^T$, and the safety regressor is $\psi(x) = 2(x - x_{\text{obs}})^T$. Inserting these into the CLF-CBF-QP (28)–(30) yields the optimization

$$(u_*(x, \hat{\theta}), \delta_*(x, \hat{\theta})) = \underset{(u, \delta) \in \mathbb{R}^2 \times [0, \infty)}{\operatorname{argmin}} \quad \frac{1}{2} \|u - u_n\|^2 + \rho \delta^2, \quad (79)$$

$$\text{s.t.} \quad 2(x - x_{\text{obs}})^T (u + \hat{\theta}) \geq -\alpha(h(x)), \quad (80)$$

$$2(x - x_d)^T (u + \hat{\theta}) \leq -\lambda V(x) + \delta, \quad (81)$$

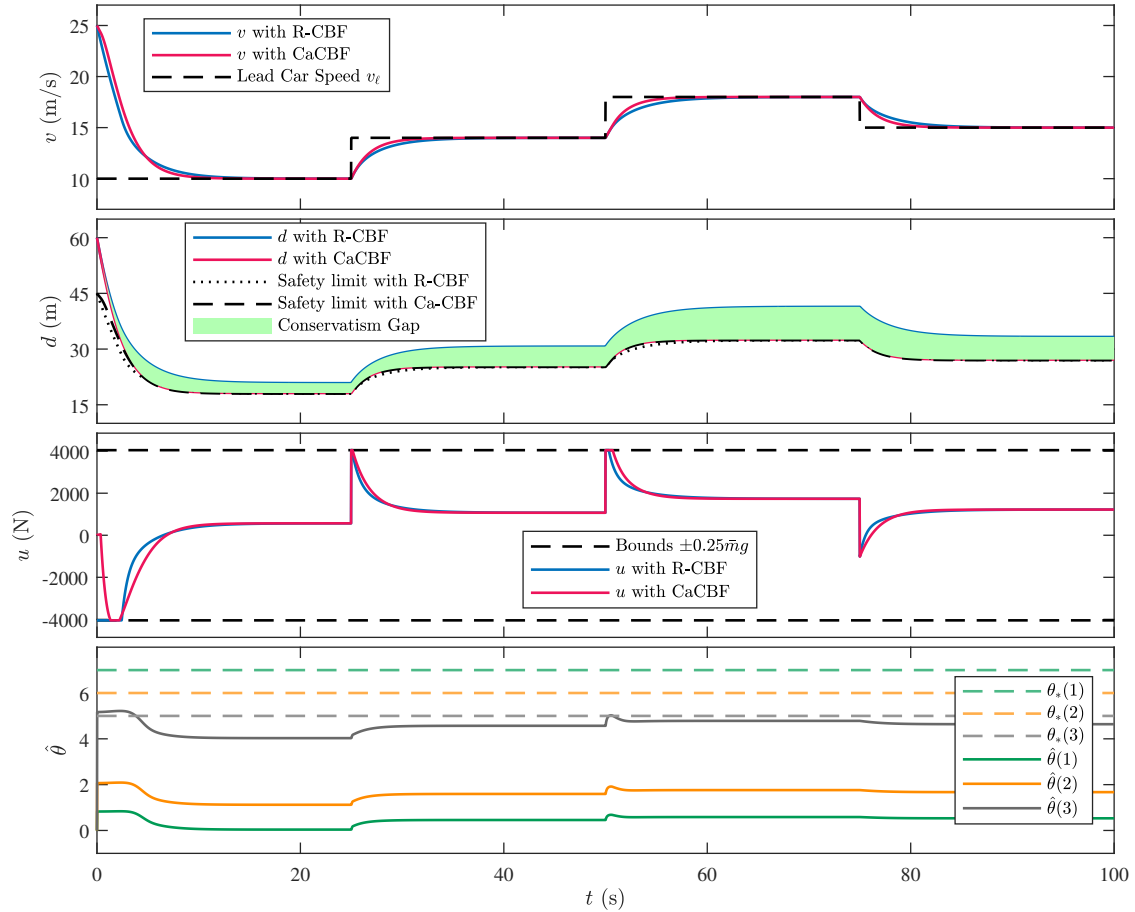


Figure 2: Example 1: Simulation results for the adaptive cruise control with unknown resistance force. The top subplot shows that the proposed CaCBF (red) tracks the desired speed more effectively than the R-CBF (blue), which exhibits spurious braking. The second subplot tracks the inter-vehicle distance d , where the green shaded region visualizes the *conservatism gap*: the robust controller maintains an unnecessary buffer due to worst-case assumptions, whereas the adaptive controller operates closer to the effective safety limit $1.8v$. The third subplot plots the control effort u , revealing that while both controllers strike the actuation boundaries (dashed black lines), they do so for distinct reasons. The R-CBF is forced into saturation by its conservative worst-case margins, whereas the CaCBF leverages braking authority to maximize tracking performance while remaining strictly safe. The bottom subplot confirms that the parameter estimates $\hat{\theta}$ (solid) need not converge perfectly to the true values θ_* (dashed) to guarantee safety.

where u_n is a nominal proportional controller and the penalty weight is $\rho = 10^3$. We set the bounds and gains as $\theta_{\max} = 1$, $\hat{\theta}(0) = 0$, $\Gamma = 20I_2$, $\gamma = 10$, and $\kappa = 1$.

For comparison, we implement a standard R-CBF. We use a fixed parameter estimate $\theta_e = 0$. To guarantee safety against all $\theta \in \Theta$, the robust controller subtracts a margin proportional to the worst-case uncertainty. Substituting the specific geometry of the obstacle into (64) generates the constraint

$$2(x - x_{\text{obs}})^T u - 2\|x - x_{\text{obs}}\|\theta_{\max} \geq -\alpha(h(x)), \quad (82)$$

which replaces (80) in the QP formulation.

Figure 3 compares the performance of both controllers. While both methods successfully reach the target without collision, the R-CBF is forced to take a wider, inefficient path. The robust controller maintains an excessive safety buffer due to its worst-case assumption that the wind might always push the robot toward the obstacle. In contrast, the adaptive controller learns the drift profile online, allowing it to operate safely with a minimal buffer. By identifying the true wind vector, the CaCBF tracks the obstacle boundary closely, reducing the deviation from the nominal straight-line path and demonstrating the efficiency gains of the proposed framework.

We quantify performance using four metrics: the minimum safety margin $h_{\min} \triangleq \min_t h(x(t))$; the total path length $\ell_{\text{path}} \triangleq \int_0^T \|u(t)\| dt$, where $T = 100$ s is the total simulation duration; the time to reach the target $T_{\text{reach}} \triangleq \min\{t \geq 0 : \|x(t) - x_d\| \leq 0.5\}$; and the time-averaged clearance $\eta \triangleq \frac{1}{T} \int_0^T h(x(t)) dt$. The metrics highlight the operational advantage of the CaCBF approach. While both controllers complete the mission, the R-CBF maintains a larger minimum margin of $h_{\min} = 0.42$ m, which forces it onto a longer path $\ell_{\text{path}} \approx 47.72$ m and results in a later arrival time of $T_{\text{reach}} = 8.40$ s. In contrast, the CaCBF safely utilizes the available space, operating with a much smaller margin of $h_{\min} = 0.04$ m, which allows for a tighter trajectory $\ell_{\text{path}} \approx 46.97$ m and faster target convergence in $T_{\text{reach}} = 7.42$ s. This reduction in conservatism is further confirmed by the average clearance metric: R-CBF operates with a wide margin $\eta = 0.79$ m, whereas CaCBF reduces conservatism to $\eta = 0.52$ m, demonstrating that the system recovers the safe operating space that the R-CBF discards. \diamond

Example 3. *Planar drone subject to unknown crosswind navigating a passage.* We illustrate the capability of the framework to handle complex safety landscapes using a passage scenario. A planar drone modeled as a double integrator must navigate through a tight gate formed by two obstacles while subject to a strong, unknown crosswind. Let the state be $x = [p^T \ v^T]^T \in \mathbb{R}^4$, where $p \in \mathbb{R}^2$ is position and $v \in \mathbb{R}^2$ is velocity. The dynamics is given by

$$\dot{x} = \begin{bmatrix} v \\ 0 \end{bmatrix} + \begin{bmatrix} 0 \\ \frac{1}{\bar{m}}I_2 \end{bmatrix} \theta_* + \begin{bmatrix} 0 \\ \frac{1}{\bar{m}}I_2 \end{bmatrix} u, \quad (83)$$

where $\bar{m} = 1$ kg is the mass, $u = [u_1 \ u_2]^T \in \mathbb{R}^2$ is the thrust control input, and $\theta_* = [1 \ 1.5]^T$ represents the unknown constant wind force. The objective is to travel from $p(0) \triangleq [-8 \ 6]^T$ to $p_d \triangleq [8 \ -6]^T$. The initial velocity is $v(0) = [0 \ 0]^T$. The gate is defined by two circular obstacles centered at $c_1 \triangleq [-5 \ 0]^T$ and $c_2 \triangleq [5 \ 0]^T$, both with radius $r \triangleq 4.8$ m. This creates a physical gap of only 0.4 m at the narrowest point, which is the origin. The safety set \mathcal{C} is the intersection of the safe regions for both obstacles, defined by the functions

$$\bar{h}_i(x) = \|p - c_i\|^2 - r^2, \quad i \in \{1, 2\}. \quad (84)$$

We bound the control input magnitude such that, for all $t \geq 0$,

$$\|u_i(t)\| \leq 10 \text{ N, for } i = 1, 2. \quad (85)$$

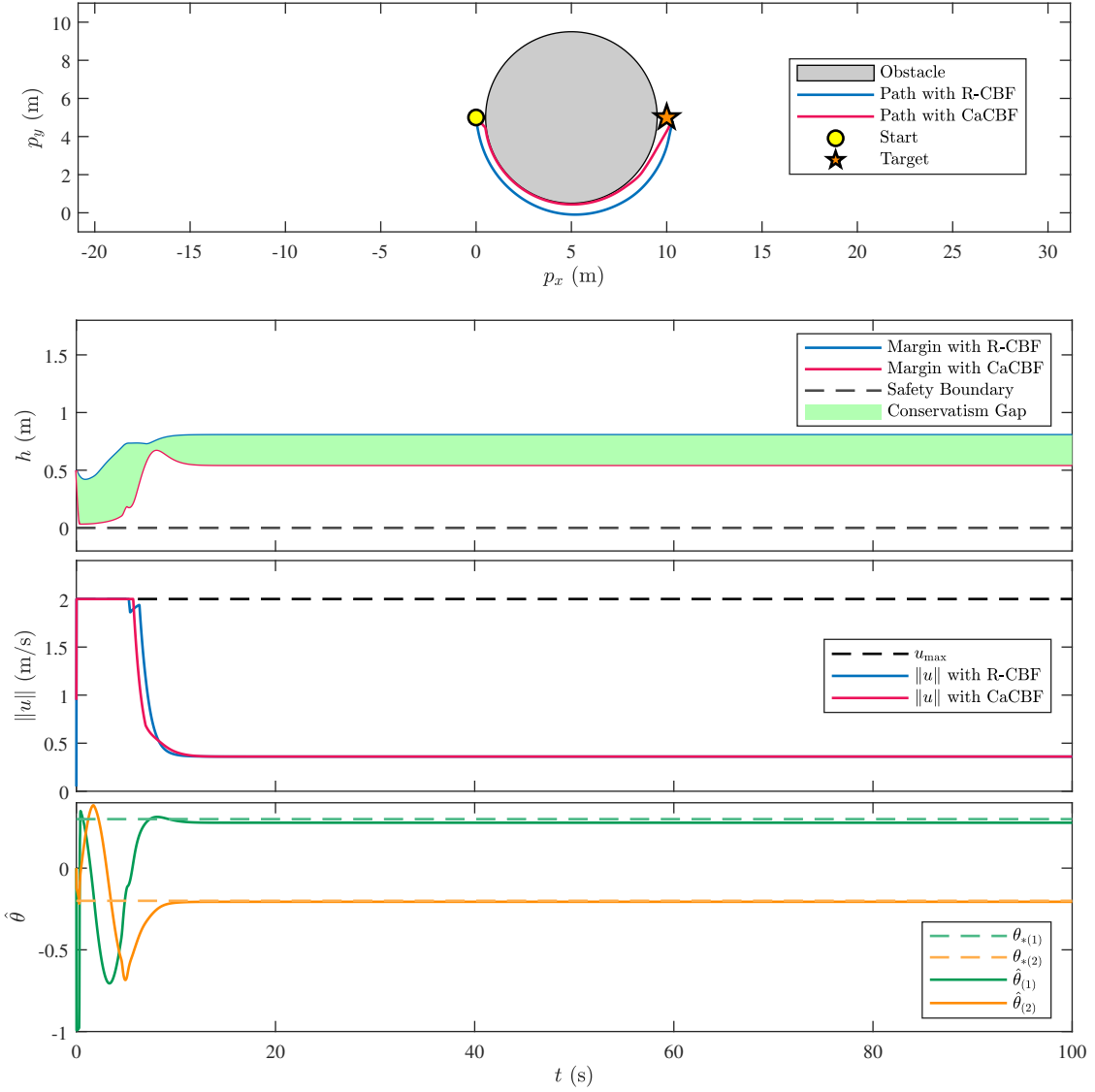


Figure 3: Example 2: Simulation results for the omnidirectional robot navigation with unknown drift. The top subplot shows the 2D trajectories: while both controllers reach the target (star), the R-CBF (blue) takes a longer route to maintain a robust margin against worst-case drift, whereas the CaCBF (red) adapts to the true drift and hugs the obstacle boundary efficiently. The second subplot tracks the safety margin $h(x)$, where the green shaded region visualizes the *conservatism gap*: R-CBF maintains a larger buffer $h_{\min} = 0.42$ m than the adaptive controller buffer $h_{\min} = 0.04$ m. The third subplot confirms that the control inputs remain within the saturation limit $\|u\| \leq 2$ m/s. The bottom subplot shows the parameter estimates $\hat{\theta}$ (solid) converging toward the true drift values θ_* (dashed), which enables the CaCBF to safely reduce the conservatism gap.

Since the position constraints \bar{h}_i have relative degree 2 with respect to the input, we employ the backstepping approach [6, 30]. We define the extended barrier functions $h_i(x) \triangleq \dot{\bar{h}}_i(x) + 2\bar{h}_i(x)$. We first implement the proposed CaCBF. We utilize a nominal PD controller $u_n \triangleq 4(p_d - p) - 4v$ to drive the drone toward p_d . We select the CLF candidate $V(x) = \frac{1}{2}\|v + p - p_d\|^2$ based on the error states to enforce convergence with a nominal rate $\lambda = 1$. We explicitly calculate the safety Lie derivatives $L_G h_i = \frac{2}{m}(p - c_i)^\top$ and the regressor $\psi_i(x) = \frac{2}{m}(p - c_i)^\top$. Inserting these into the CLF-CBF-QP (28)–(30) yields the optimization

$$(u_*(x, \hat{\theta}), \delta_*(x, \hat{\theta})) = \underset{(u, \delta) \in \mathbb{R}^2 \times \mathbb{R}}{\operatorname{argmin}} \quad \frac{1}{2}\|u - u_n\|^2 + \rho\delta^2 \quad (86)$$

$$\text{s.t.} \quad \frac{2}{m}(p - c_i)^\top(u + \hat{\theta}) + 2\|v\|^2 + 14(p - c_i)^\top v \geq -10\bar{h}_i(x), \quad \text{for all } i \in \{1, 2\}, \quad (87)$$

$$\frac{1}{m}(v + p - p_d)^\top(u + \hat{\theta}) + (v + p - p_d)^\top v \leq -\lambda V(x) + \delta, \quad (88)$$

where the class \mathcal{K} function is $\alpha(h) = 5h$ and the penalty weight is $\rho = 10^3$. We set the bounds and gains as $\theta_{\max} = 3$, $\hat{\theta}(0) = 0$, $\Gamma = 10I_2$, and implement CaCBF.

For comparison, we implement R-CBF using a fixed estimate $\theta_e = 0$. To guarantee safety against all $\theta \in \Theta$, the robust controller subtracts a margin proportional to the worst-case uncertainty. Substituting the specific geometry into the robust condition yields the constraints

$$2(p - c_i)^\top u - 6\|p - c_i\| + 2\|v\|^2 + 14(p - c_i)^\top v \geq -10\bar{h}_i(x), \quad \text{for all } i \in \{1, 2\}, \quad (89)$$

which replace (87) in the QP formulation. Figure 4 illustrates the critical limitation of the robust approach. The R-CBF assumes the worst-case wind could push the drone into the walls, mathematically inflating the obstacles by a robust margin, which is visualized as dotted lines. In this scenario, these margins overlap, effectively closing the gate. Consequently, R-CBF perceives the passage as impassable and braking to a halt before entering the gap. In contrast, the CaCBF learns the true wind profile, allowing it to shrink the safety margins dynamically. By adapting to the true wind forces, CaCBF identifies the passage as safe and successfully navigates through the passage.

We quantify performance using four metrics: the minimum safety margin

$$h_{\min} \triangleq \min_{t \in [0, T]} \left(\min_{i \in \{1, 2\}} \bar{h}_i(x(t)) \right)^{1/2};$$

the total control effort $E_{\text{control}} \triangleq \int_0^T \|u(t)\| dt$; the time to reach the target T_{reach} ; and the average clearance $\eta \triangleq \frac{1}{T} \int_0^T h_{\min}(t) dt$, where $T = 12$ s is the simulation duration. The results confirm the topological advantage of CaCBF. The R-CBF maintains a larger clearance $h_{\min} = 0.22$ m and $\eta = 0.35$ m because the constraints preclude entry into the gap, resulting in a failed mission (i.e., timeout at $T_{\text{reach}} = 12$ s). The CaCBF, by contrast, operates with a much tighter margin $h_{\min} = 0.04$ m to successfully traverse the bottleneck. Consequently, the CaCBF controller utilizes higher control effort $E_{\text{control}} \approx 40.11$ N·s compared to the R-CBF control effort $E_{\text{control}} \approx 29.03$ N·s as CaCBF performs the necessary maneuvers to complete the mission that is infeasible for R-CBF. \diamond

7 Conclusion and Future Work

This work introduced the composite adaptive control barrier function (CaCBF) to reconcile safety guarantees with parametric uncertainty. By deriving the adaptation law from a unified energy function, one that integrates prediction error with the safety barrier, the framework ensures the system actively dissipates the

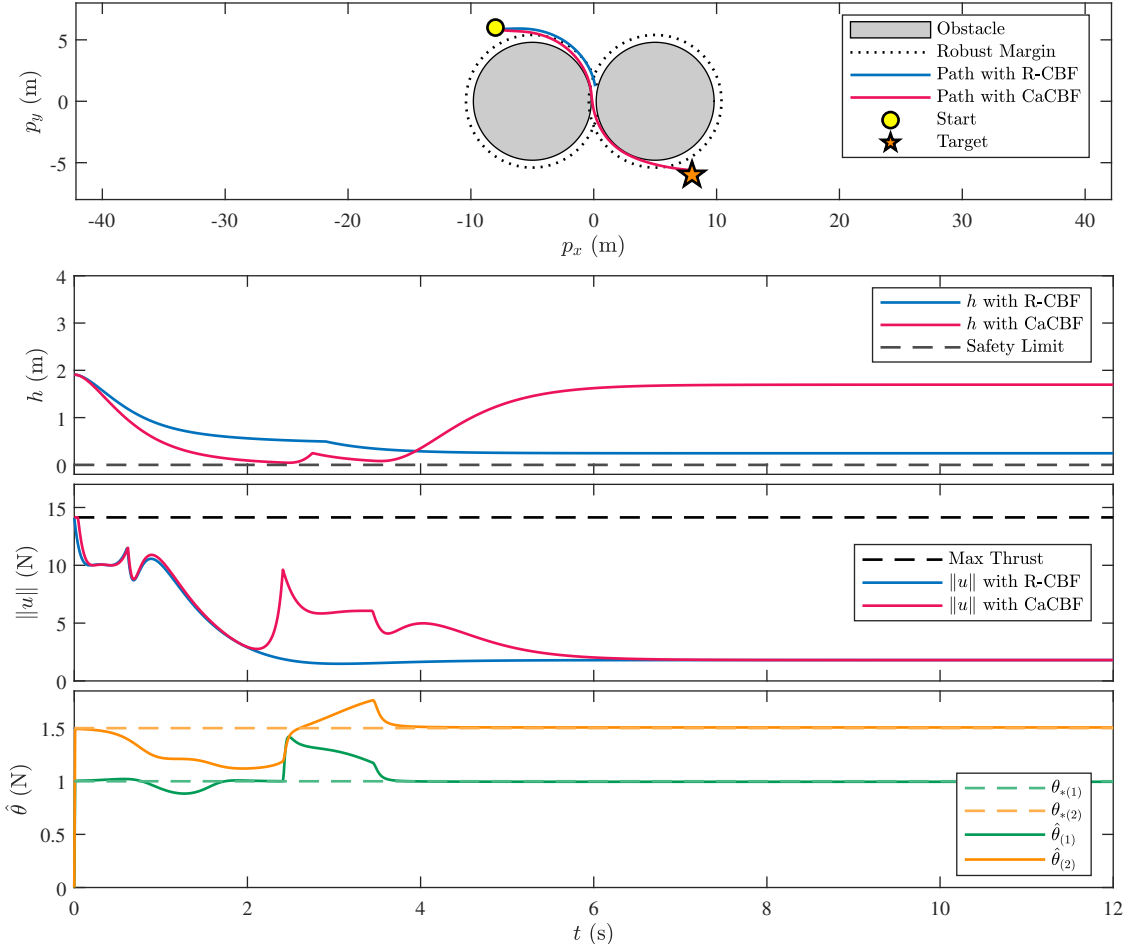


Figure 4: Example 3: Simulation results for the planar drone subject to unknown crosswind navigating a passage. The top subplot shows the trajectories, where the R-CBF (blue) is blocked because the robust margins (dotted) of the two obstacles overlap, effectively closing the gate. The CaCBF (red) learns the wind parameters, shrinks these margins, and successfully passes through the gap to reach the target (star). The second subplot tracks the minimum distance to the nearest wall, confirming that the CaCBF safely utilizes the available space ($h > 0$). The third subplot shows the control effort $\|u\|$, illustrating the maneuvering required to pass the gate. The bottom subplot confirms the convergence of the parameter estimates $\hat{\theta}$ (dotted) toward the true wind values θ_* (dashed).

energy required to breach safety constraints. This coupling guarantees the forward invariance of the safe set without the conservatism inherent to worst-case bounds. Simulations of adaptive cruise control, an omnidirectional robot, and a planar drone demonstrate that the controller dynamically adjusts safety margins as estimates converge, recovering the performance lost by robust methods while enforcing strict safety.

Future research must address the assumptions of the current framework. Extending the method to unstructured dynamics may require universal approximators, such as neural networks or kernel methods, to learn residual terms online. Furthermore, while the current quadratic program handles input constraints, ensuring recursive feasibility under large initial parameter errors remains an open theoretical challenge. Finally, potential extensions for real-world deployment include the development of output-feedback observers to handle partial state information and experimental validation on hardware platforms to assess robustness against environmental noise.

References

- [1] Aaron D Ames, Samuel Coogan, Magnus Egerstedt, Gennaro Notomista, Koushil Sreenath, and Paulo Tabuada. Control barrier functions: Theory and applications. *European Control Conference*, pages 3420–3431, 2019.
- [2] Aaron D Ames, Xiangru Xu, Jessy W Grizzle, and Paulo Tabuada. Control barrier function based quadratic programs for safety critical systems. *IEEE Transactions on Automatic Control*, 62(8):3861–3876, 2016.
- [3] Mrdjan Jankovic. Robust control barrier functions for constrained stabilization of nonlinear systems. *Automatica*, 96:359–367, 2018.
- [4] Pan Zhao, Yanbing Mao, Chuyuan Tao, Naira Hovakimyan, and Xiaofeng Wang. Adaptive robust quadratic programs using control Lyapunov and barrier functions. *IEEE Conference on Decision and Control*, pages 5749–5754, 2020.
- [5] Jyot Buch, Shih-Chi Liao, and Peter Seiler. Robust control barrier functions with sector-bounded uncertainties. *IEEE Control Systems Letters*, 6:1994–1999, 2022.
- [6] Wei Xiao and Calin Belta. High-order control barrier functions. *IEEE Transactions on Automatic Control*, 67(7):3655–3662, 2021.
- [7] Kemin Zhou and John Comstock Doyle. *Essentials of Robust Control*. Prentice Hall, Upper Saddle River, NJ, 1998.
- [8] Ersin Daş and Joel W Burdick. Robust control barrier functions using uncertainty estimation with application to mobile robots. *IEEE Transactions on Automatic Control*, 2025.
- [9] Sarah Dean, Andrew J Taylor, Ryan K Cosner, Benjamin Recht, and Aaron D Ames. Guaranteeing safety of learned perception modules via measurement-robust control barrier functions. *Conference on Robot Learning*, pages 654–670, 2021.
- [10] Lennart Ljung. *System Identification: Theory for the User*. Prentice Hall PTR, Upper Saddle River, NJ, 1999.
- [11] Andrew J Taylor and Aaron D Ames. Adaptive safety with control barrier functions. *American Control Conference*, pages 1399–1405, 2020.

- [12] Brett T Lopez and Jean-Jacques E Slotine. Unmatched control barrier functions: Certainty equivalence adaptive safety. *IEEE Control Systems Letters*, 7:1–6, 2023.
- [13] Wei Xiao, Calin Belta, and Christos G Cassandras. Adaptive control barrier functions. *IEEE Transactions on Automatic Control*, 67(5):2267–2281, 2022.
- [14] Max H Cohen and Calin Belta. High order robust adaptive control barrier functions and exponentially stabilizing adaptive control Lyapunov functions. *American Control Conference*, pages 2502–2507, 2022.
- [15] Yifan Cheng, Yuxiang Zhang, Hongqing Chu, Qiankun Yu, Bingzhao Gao, and Hong Chen. Safety-critical control of 4WDEV trajectory tracking via adaptive control barrier function. *IEEE Transactions on Transportation Electrification*, 10(4):10361–10373, 2024.
- [16] Yuxiang Zhang, Shuzhi Sam Ge, Xiaoling Liang, Bernard Voon Ee How, and Hong Chen. Safety-critical automated surface vessels MIMO control with adaptive control barrier functions under model uncertainties. *IEEE Transactions on Automation Science and Engineering*, 22:17253–17264, 2025.
- [17] Yifan Cheng, Yuxiang Zhang, Yifei Wang, Hongqing Chu, Bingzhao Gao, and Hong Chen. Resilient safety-critical control for autonomous electric vehicles via disturbance-observer-based adaptive control barrier functions. *Control Engineering Practice*, 169:106690, 2026.
- [18] Ricardo Gutierrez and Jesse B. Hoagg. Adaptive control barrier functions with vanishing conservativeness under persistency of excitation. *arXiv preprint arXiv:2411.12899*, 2024.
- [19] Brett T Lopez, Jean-Jacques E Slotine, and Jonathan P How. Robust adaptive control barrier functions: An adaptive & data-driven approach to safety. *IEEE Control Systems Letters*, 5(3):1031–1036, 2020.
- [20] Danping Zeng, Yiming Jiang, Yaonan Wang, Hui Zhang, and Yun Feng. Robust adaptive control barrier functions for input-affine systems: Application to uncertain manipulator safety constraints. *IEEE Control Systems Letters*, 8:279–284, 2024.
- [21] Ricardo Gutierrez and Jesse B. Hoagg. Control barrier functions with real-time Gaussian process modeling. *arXiv preprint arXiv:2505.06765*, 2025.
- [22] Alaa Eddine Chriat and Chuangchuang Sun. On the optimality, stability, and feasibility of control barrier functions: An adaptive learning-based approach. *IEEE Robotics and Automation Letters*, 8(11):7865–7872, 2023.
- [23] Tingting Jiang, Jinkun Liu, and Wei He. Adaptive boundary control for a flexible manipulator with state constraints using a barrier Lyapunov function. *ASME Journal of Dynamic Systems, Measurement, and Control*, 140(8):081018, 2018.
- [24] Andrea L’Afflitto. Barrier Lyapunov functions and constrained model reference adaptive control. *IEEE Control Systems Letters*, 2(3):441–446, 2018.
- [25] Victor Hugo Pereira Rodrigues, Liu Hsu, Tiago Roux Oliveira, and Leonid Fridman. Adaptive sliding mode control with guaranteed performance based on monitoring and barrier functions. *International Journal of Adaptive Control and Signal Processing*, 35(7):1271–1292, 2021.
- [26] Hao An, Hongwei Xia, and Changhong Wang. Barrier Lyapunov function-based adaptive control for hypersonic flight vehicles. *Nonlinear Dynamics*, 88:1833–1853, 2017.

- [27] Miroslav Krstić, Ioannis Kanellakopoulos, and Petar V Kokotović. *Nonlinear and Adaptive Control Design*. John Wiley & Sons, 1995.
- [28] Shankar Sastry and Marc Bodson. *Adaptive Control: Stability, Convergence and Robustness*. Courier Corporation, 2011.
- [29] Petros A Ioannou and Jing Sun. *Robust Adaptive Control*. Courier Corporation, 2012.
- [30] Quan Nguyen and Koushil Sreenath. Exponential control barrier functions for enforcing high relative-degree safety-critical constraints. *American Control Conference*, pages 322–328, 2016.
- [31] Benjamin Morris, Michael J Powell, and Aaron D Ames. Sufficient conditions for the Lipschitz continuity of QP-based multi-objective control of humanoid robots. *IEEE Conference on Decision and Control*, pages 2920–2926, 2013.